Highlights on Spanish Astrophysics IX, Proceedings of the XII Scientific Meeting of the Spanish Astronomical Society held on July 18 – 22, 2016, in Bilbao, Spain. S. Arribas, A. Alonso-Herrero, F. Figueras, C. Hernández-Monteagudo, A. Sánchez-Lavega, S. Pérez-Hoyos (eds.)

An X-ray study of the lower-luminosity LIRGs from GOALS

N. Torres-Albà[1], K. Iwasawa[1,2],

[1] Institut de Ciències del Cosmos (ICCUB), Universitat de Barcelona (IEEC-UB), Martí i Franquès, 1, 08028 Barcelona, Spain
[2] ICREA, Pg. Lluís Companys 23, 08010 Barcelona, Spain

Abstract

We present Chandra observations for a sample of 59 Luminous Infrared Galaxies (LIRGs) from the lower-luminosity portion of the Great Observatory All-sky LIRG Survey (GOALS). The GOALS is a multiwavelegth study of the most luminous IR-selected galaxies in the local Universe, and this X-ray study, complimenting the previous work on the higher-luminosity sample, benefits from the imaging and spectroscopic data from HST, Spitzer and Herschel. With combined X-ray and mid-infrared diagnostics, AGN are found in 33% of the galaxies in the sample, a fraction lower than that found for the higher luminosity sample. The correlation study of far-IR and X-ray emission shows that the GOALS galaxies without traces of AGN appear to be underluminous in X-ray, compared to the previously studied star-forming galaxies with lower star formation rates. Results on X-ray spectral study of the sample will also be presented.

1 Introduction

Luminous infrared galaxies (LIRGs) are galaxies with an infrared luminosity between $10^{11} L_{\odot}$ and $10^{12} L_{\odot}$, emitting more in this band than in all other bands combined. Galaxies with infrared luminosity above $10^{12} L_{\odot}$ are called ULIRGs, Ultra Luminous Infrared Galaxies.

The Great Observatories All-sky LIRG Survey (GOALS, [1]), is combining imaging and spectroscopic data from NASA's Spitzer, Hubble, Chandra and GALEX space-borne observatories in a comprehensive study of over 200 of the most luminous infrared-selected galaxies in the local Universe.

This work directly benefits from Hubble Space Telescope imaging data, used as a visual support for Chandra X-ray contours. Spitzer and Herschel infrared data are used to determine the IR luminosity of the sample's galaxies, as well as determining the contribution to the total

output of each galaxy in multiple systems. Spitzer spectroscopy data are also used as a criteria to determine the AGN fraction in the sample.

The objects in GOALS are a complete subset of the IRAS Revised Bright Galaxy Sample (RBGS, [11]), which contains the brightest 60-micron sources in the extragalactic sky. The LIRGs and ULIRGs targeted in GOALS span the full range of nuclear spectral types (type 1 and 2 AGN, LINERs, and starbursts) and interaction stages (major and minor mergers, and isolated galaxies). They provide an unbiased picture of the processes responsible for enhanced infrared emission in the local Universe, and are excellent analogues for comparisons with infrared and sub-millimetre selected galaxies at high-redshift.

The sample studied in this work consists of 59 systems from the GOALS sample, 20 of which contain multiple galaxies. It represents the low-luminosity part of the GOALS sample, with 11.05 $\leq \log(L_{ir}/L_{\odot}) \leq$ 11.73, incomplete as Chandra data for all systems is unavailable. The redshift range is $z = 0.003 - 0.037$. A complete study of the high-luminosity part, 11.73 $\leq \log(L_{ir}/L_{\odot}) \leq$ 12.57, with 44 systems, was carried out by [6], with $z = 0.010 - 0.088$.

Through the X-ray study of the sample, the AGN fraction is estimated, X-ray fluxes are obtained through spectral fitting, and a comparison of X-ray to infrared luminosity is performed. All results are compared to the ones obtained previously for the high luminosity sample.

2 AGN selection

The main source of infrared luminosity in a U/LIRG is the central starburst, which may be triggered by a gas-rich galaxy merger. The initial, completely obscured U/LIRG would disperse or consume the gas and evolve into and obscured quasar (QSO), and eventually into an exposed QSO (e.g. [4], [10]). This will eventually lead to the formation of an elliptical galaxy, and account for the growth of the central supermassive black hole (e.g. [12], [3]). Therefore, the QSO phase would always a phase of galaxy evolution, coincident with the U/LIRG stage. In order to validate this theory, we check the AGN fraction in our sample.

For dusty objects such as LIRGs, X-ray AGN diagnosis is specially adequate, as X-rays are much less absorbed than optical frequencies. Galaxies with a hardness ratio higher than -0.3 (defined as $HR = (H-S)/(H+S)$, where H and S are the background-corrected counts in the 2−8 keV and 0.5−2 keV bands, respectively), presence of the 6.4 Fe K line and/or absorbed AGN features, are classified as AGN. This criteria was derived by [6] for the high luminosity sample. Spectral features are also used for the diagnosis, examples of which can be found in Section 3.

We also use the presence of the [Ne v] 14.2 μm line in Spitzer IRS spectra [8] as a diagnostic criterion, which traces ionization gas. The ionization potential of [Ne v] is 96 eV, too high to be produced by OB stars, and therefore associated to AGN presence.

From the 79 objects in the sample, 26 show signs from AGN presence either in the infrared spectroscopy, through the presence of the [Ne v] or in X-rays (see Table 1). This represents a 33% of our sample, lower than the 50% found for the high-luminosity sample [6].

No. (1)	**Name** (2)	**VO** (3)	**YKS** (4)	**D_{agn}** (5)	**[Ne v]** (6)	**6.2 μm EQW** (7)	**X-ray (CLA)** (8)
45	UGC 08387	L	cp	0.5	Y	N	N
57	F06076-2139(S)	-	-	-	N	N	C
64	III Zw 035 (S)	L	S2	0.7	N	-	C
67	F16399-0937(S)	-	cp	0.2	N	N	C
68	16164-0746	L	S2	0.7	Y	N	C
71	NGC 2623	-	-	-	Y	N	C
72	IC 5298	-	-	-	Y	N	A
79	NGC 5256 (NE)	S2	S2	0.7	Y(u)	N	A
79	NGC 5256 (SW)	L	cp	0.6	Y(u)	N	N
85	F17138-1017	-	-	-	N	N	C
100	NGC 7130	L	S2	0.9	Y	N	L
105	NGC 7592 (E)	H	H	0	Y(u)	N	N
105	NGC 7592 (W)	S2	S2	0.7	Y(u)	N	N
107	NGC 4922 (N)	L(u)	S2(u)	0.6(u)	Y	N	A
114	NGC 0232	H	cp	0.4	Y	N	N
120	CGCG 049-057	-	-	-	N	N	C
121	NGC 1068	S2	S2	1	Y	-	L
127	MCG-03-34-064	-	H	0	Y	Y	AL
136	MCG-01-60-022	-	-	-	N	-	CA
142	NGC 5135	-	S2	0.8	Y	N	LA
144	IC 0860	-	-	-	N	N	C
169	ESO 343-IG13 (N)	H	cp	0.2	N	N	C
191	ESO 420-G13	-	H	0.4	Y	N	N
194	ESO 432-IG6 (NE)	-	-	-	N	N	A
194	ESO 432-IG6 (SW)	-	-	-	N	N	A
198	NGC 1365	-	-	-	N	N	CLA

Table 1: Table of AGN diagnostics. (1) Number of the object as in [1]. (2) Galaxy name. (3) Optical class as in [13]. (4) Optical class from [14]. (5) AGN fraction, see [14] for details. (6) Detection of [Ne v] 14.32 μm from [8]. (7) X-ray evidence of AGN presence through Chandra spectrum analysis; C: X-ray colour (HR $\geq$ -0.3), L: 6.4 keV Fe K line, A: absorbed AGN feature. (u) stands for "unresolved" in a double system.

3 Spectral study

From the spectral study of the sample, through spectral fitting, the X-ray luminosities can be determined. Those are used in Section 4 to compare with far infrared luminosities.

AGN diagnostics are also obtained from the spectra. Clear signatures of heavily obscured AGN are an absorbed, luminous emission in X-rays, or the presence of a strong Fe K line at 6.4 keV.

In Fig. 1 we present three illustrative spectra. The typical X-ray spectra for a starburst galaxy, NGC 3256, doesn't trigger any of the X-ray AGN selection criteria described in Section 2. MCG-03-34-064, on the other hand, is classified as an AGN through two of the X-ray criteria: the Fe Kα line and the absorbed AGN feature. This last feature is recognisable as a high increase of X-ray flux at higher energies. NGC 5135 presents a high energy excess,

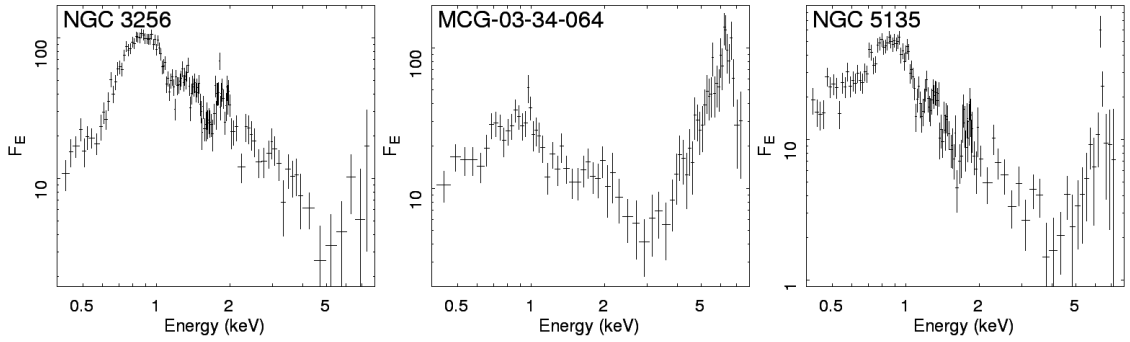

Figure 1: Chandra X-ray spectrum of the starburst galaxy NGC 3256, the absorbed AGN MCG-03-34-064 and NGC 5135, for which there is marginal evidence of AGN.

which can be fitted as an iron line at 6.41 keV. It is interpreted as marginal evidence for AGN presence, due to the limited amount of counts detected by Chandra at high energies.

The triggered X-ray AGN selection criteria are specified for all AGN in the sample in Table 1.

All the presented spectra have been corrected for detector response and converted into flux density units.

4 Correlation between IR and X-ray emission in LIRGs

In astronomy, many methods are used to estimate the star formation rate in galaxies, the basis of which is quantifying the amount of hot, young and short-lived stars. One of these methods is a measurement of the energy deposed in the dust of the interstellar medium by these stars, which is obtained through far-infrared luminosity measurements. Therefore, far-infrared luminosity can be directly related to the star formation rate.

In galaxies with a considerable amount of star formation, such as starburst galaxies, emission in other wavelengths can be somewhat related to young and massive stars, such as X-ray luminosity (e.g. X-ray binaries emission, supernova remnants (SNRs)). Therefore, it has been suggested that if a good correlation between X-ray luminosity and IR luminosity exists in galaxies, the star formation rate (SFR) can be directly inferred from the X-ray luminosity (e.g. [9], [2], [7]). However, the applicability of this method has been questioned due to experimental results for LIRGs at higher SFRs (e.g. [5]).

In Fig. 2, X-ray luminosity is plotted as a function of infrared luminosity for the LIRGs in GOALS. The open symbols correspond to the galaxies in the low-luminosity sample analysed in this work, the red symbols are the galaxies analysed in [6], and the dashed line is the correlation derived by [9] for lower-luminosity starburst galaxies. As an AGN can actively contribute to both X-ray and infrared luminosities, thus introducing a contamination into this relation, galaxies classified as AGN (see this work's Table 1 and Table 5 from [6]) have been removed.

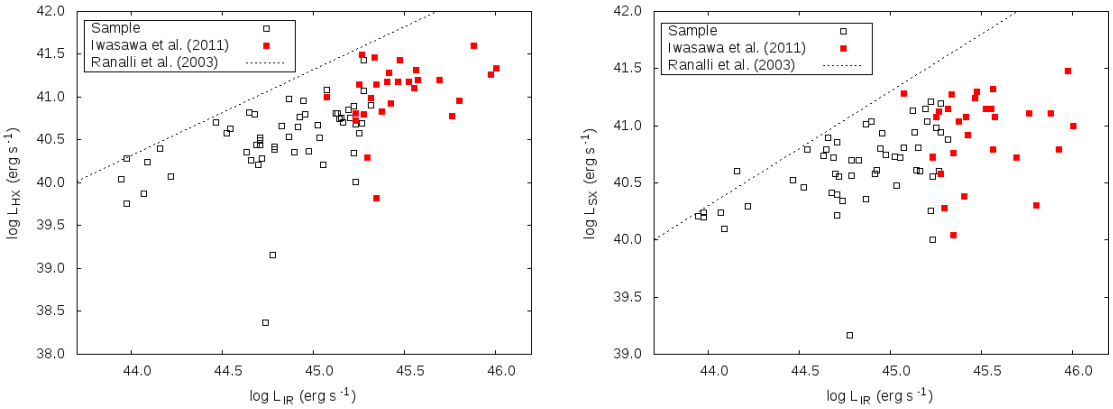

Figure 2: X-ray luminosity in hard band, $2-7$ keV, (left) and soft band, $0.5-2$ keV, (right) versus the far infrared luminosity (FIR) (calculated as in [9]), for both the galaxies in the present sample and the galaxies in the high luminosity sample [6]. The dashed line shows the correlation derived by [9] for galaxies at lower infrared luminosities.

As seen in Fig. 2, LIRGs and ULIRGs deviate from the correlation found at lower luminosities, and appear to be underluminous in X-rays, with this trend increasing as infrared luminosity increases. Also, the plotted data shows high dispersion.

5 Conclusions and future work

When analysing the GOALs' LIRGs in X-rays, together with the results derived from infrared spectroscopy, a 33% of AGN presence is found in the low-luminosity sample, and a 50% was found in the high-luminosity sample analysed by [6]. This shows a tendency for AGN presence to increase with infrared luminosity.

Plotting the X-ray luminosity versus the infrared luminosity for these U/LIRGs shows a deviation from the correlation found for starburst at lower infrared luminosities, and high dispersion. A possible explanation for both facts is that U/LIRGs mostly contain AGN, and that though it is possible to detect some of them and eliminate them from the correlation, the most enshrouded ones are completely absorbed in X-rays, and therefore also optical, and thus mostly undetectable to us.

These highly obscured AGN would not contribute to the X-ray luminosity, but their high-energy photons would be absorbed by dust particles and re-emitted in the infrared, thus contributing to the FIR emission. Also, since the level of obscuration and AGN brightness is different for every galaxy, this can also explain the high dispersion.

Results for the spectral analysis of the whole low-luminosity sample will soon be published, and an analysis for the remaining $\sim$100 LIRGs in GOALs will be performed as soon as data is available, in order to increase the statistical significance of the derived results.

Acknowledgments

We aknowledge support by the Spanish Ministerio de Economa y Competitividad (MINECO/FEDER, UE) through MDM-2014-0369 of ICCUB (Unidad de Excelencia 'María de Maeztu'). N.T-A also aknowledges support from MINECO under grants AYA2013-47447-C3-1-P and FPU14/04887 grant. K.I. also acknowledges support from MINECO under grant AYA2013-47447-C3-2-P.

References

[1] Armus, L., Mazzarella, J., Evans, A., et al. 2009, PASP, 121, 559A

[2] Grimm, H.-J., Gilfanov, M. & Sunyaev, R. 2003, MNRAS, 339, 793G

[3] Hopkins, P.F,, Bundy, K., Murray, N. et al. 2009, MNRAS, 398, 898

[4] Hopkins, P.F., Hernquist, L., Cox, T.J., et al. 2005, ApJ, 630, 705H

[5] Iwasawa, K., Sanders, D.B., Evans, A.S., et al. 2009, ApJ, 695L, 103I

[6] Iwasawa, K., Sanders, D.B., Teng, S.H., et al. 2011, A&A, 529A, 106I

[7] Mineo, S., Gilfanov, M., Lehmer, B.D., et al. 2014, MNRAS, 437, 1698M

[8] Petric, A.O., Armus, L., Howell, J., et al. 2011, ApJ, 730, 28P

[9] Ranalli, P., Comastri, A. & Setti, G. 2003, A&A, 399, 39R

[10] Sanders, D.B. 1999, Astrophysics and Space Science, 266, 331

[11] Sanders, D.B., Mazzarella, J.M., Kim, D.-C., et al. 2003, AJ, 126, 1607S

[12] Sanders, D.B., Soifer, B.T., Elias, J.H., et al. 1988, ApJ, 325, 74

[13] Veilleux, S., Kim, D.-C. & Sanders, D.B. 1999, ApJ, 522, 113V

[14] Yuan, T.-T., Kewley, L.J. & Sanders, D.B. 1999, ApJ, 709, 884Y